

## Performance of Interfering Strip Footings Resting on Reinforced Sand under Uniform and Nonuniform Load-Experimental and Numerical Study

Ahmed M. Eltohamy<sup>1,2</sup> ; Ahmed F. Zidan<sup>1</sup>

<sup>1</sup>Structural Engineering Department, Faculty of Engineering, Beiny Suafe University, Egypt.

<sup>2</sup> Structural Engineering Department, Faculty of Engineering, Umm Al-Qura University, Saudia Arabia.

[Ahmedzidan2008@gmail.com](mailto:Ahmedzidan2008@gmail.com)

**Abstract:** In This paper an experimental and numerical program was adopted to investigate the interface effect of shallow strip foundations constructed on homogeneous sand reinforced by geogrid. The ultimate bearing capacity of a number of multiple footings in a group becomes always greater than that of a single isolated footing. Several parameters including soil type, spacing between interfering footings and the foundation level under both uniform and eccentric vertical loads were examined. A detailed numerical analysis study was performed to investigate the effect of angle of internal friction, foundation level and load eccentricity on bearing capacity. The failure stage in the sand was controlled using hyperbolic relationship between strain and stress level. The best location of interfering footings was determined to achieve the maximum bearing capacity for closely spaced strip footings and it was found that the best clear spacing between footings was 0.4 and 0.6 times the footing width for reinforced and unreinforced sand, respectively. Some significant observations on the performance of footing-geogrid systems with change of the values of parametric study are also presented in this paper.

[Ahmed M. Eltohamy; Ahmed F. Zidan **Performance of Interfering Strip Footings Resting on Reinforced Sand under Uniform and Nonuniform Load-Experimental and Numerical Study.** *J Am Sci* 2013;9(1):421-430] (ISSN: 1545-1003). <http://www.jofamericanscience.org>. 62

**Keywords:** Adjacent footings, strip footings, sand reinforcement, eccentricity, finite element method, soil modelling.

### 1. Introduction

It is more realistic that the footings are typically constructed as a group in multiple configurations. This may cause interference between neighbouring foundations. This interference has effects on the bearing capacity, settlement, and rotation of footings subjected to vertical loads. The lateral distance of the passive zone for a footing extends approximately 3 to 5 times the footing width according to Terzaghi (1943). If an adjacent footing is placed sufficiently far beyond this lateral distance, the footing will behave as a single footing. However, if footing is implemented within this lateral distance the failure and slip mechanism of a single footing would no longer be valid. Also, the bearing capacity would differ from that obtained from the conventional bearing capacity equation. A number of studies have been performed by different investigators to determine the ultimate bearing capacity for a group of two strip footings on unreinforced soil (Stuart, 1962; Saran and Agarwal, (1974); Das and Cherif, (1983); Graham *et al.*, (1984); Kumar and Saran, (2003); Kumar and Ghose, (2007); Kumar and Kouzer, (2008); Kumar and Bhoi, (2008); Kouzer and Kumar, (2008)).

The use of reinforcement materials under footings to improve the bearing capacity and settlement behaviour became an important topic in the last decade. Both experimental and theoretical

studies have been performed by several researchers to investigate the benefits of soil reinforcing ( Chung and Cascante, (2007); Bathurst *et al.*, (2009), Alamshahi and Hataf ,(2009); Vinod *et al.*, (2009); Julie Lovisa *et al.* , (2010); Tafreshi and Dawson, (2010); Zidan, (2012).

It is understood that the ultimate bearing capacity of a number of multiple footings in a group becomes always greater than that of a single isolated footing. Graham *et el.* (1984), Kouzer and Kumar (2008). Khing *et al.* (1992), Kumar and Saran (2003) and Ghazavi and Lavasan (2008) studied interfering footings on reinforced sand. However, they did not present sufficient information about the effects of foundation level and uniformity of load carried by the interfering footings on the ultimate bearing capacity. Khing *et al.* (1992) performed experimental tests on closely spaced strip footings reinforced with a geogrid.

Ghazavi and Lavasan (2008) studied the interface effect of shallow foundations constructed on sand reinforced with geosynthetics. They explored the role of contributing parameters on the interference factor, including the reinforcement location, the number of reinforcing layers, and the distance between two close footings. In their study, the failure stage in the sand was controlled using the Mohr–Coulomb criterion and a non-associated flow rule. The results showed that the bearing capacity of

interfering footing increases with the use of geogrid layers, depending on the distance between two footings. The best geometry and orientation of the geogrid layers were determined to achieve maximum bearing capacity for closely spaced square footings. Parametric studies demonstrated that the efficiency of reinforcement on the bearing capacity of interfering footings is greater than that on an isolated reinforced footing. In addition, reinforcement caused the bearing capacity of interfering footings to increase by about 1.5 and 2 for one and two reinforcement layers, respectively.

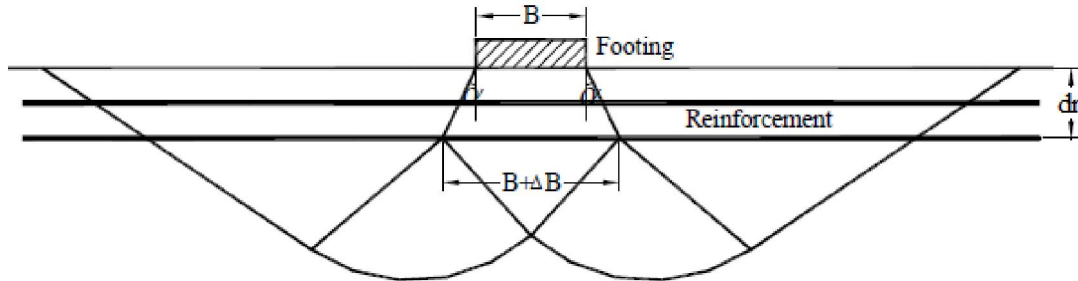


Fig.1 Failure mechanism of reinforced soil foundation after Huang and Menq, (1997)

For a strip footing resting on unreinforced soil:

$$q_{(unreinfs)} = \zeta * \gamma * B * N + \gamma * d * N_d \quad (1)$$

For a strip footing resting on reinforced soil:

$$q_{(reinf)s} = \zeta * \gamma * (B + \Delta B) * N + \gamma * d * N_d \quad (2)$$

where  $q_{(unreinfs)}$  and  $q_{(reinf)s}$  are the ultimate bearing capacity of a single strip footing resting on unreinforced and reinforced soil foundation, respectively;  $\zeta$  is a coefficient depending on footing shape;  $\gamma$  is the dry unit weight of soil;  $B$  is the width of footing;  $d$  is the depth of foundation level,  $N$  and  $N_d$  are bearing capacity factors,  $\Delta B$  is the increase of footing width due to the inclusion of reinforcement =  $(2 * d_r) \tan \alpha$ ;  $d_r$  is the vertical distance between foundation level and the deepest layer of reinforcement; and  $\alpha$  is the stress distribution angle. Based on experimental data of different researchers Huang and Menq (1997) performed regression analysis to obtain the following expression of the stress distribution angle  $\alpha$ .

$$\tan \alpha = 0.68 - 2.071 * h/B + 0.743 * CR + 0.3 * l/B + 0.076 * N \quad (3)$$

Where  $h$  is the spacing between reinforcement layers;  $CR$  is the covering ratio of reinforcement = area of reinforcement divided by area of soil covered by reinforcement.

In the present study an experimental and numerical program was adopted to investigate the interface effect of shallow foundations constructed on reinforced sand on the ultimate bearing capacity. Several parameters including soil type, spacing between interfering footings and the foundation level under both uniform and eccentric vertical loads are

Huang and Menq (1997) investigated the reinforced soil foundation system based on a failure mechanism proposed by Schlosser *et al.* (1983), as shown in Fig. 1. The basic concept which has been adopted by the researchers is that the bearing capacity of footing having a width of  $(B)$  on reinforced soil foundation is equivalent to that of a wider footing with a width of  $(B + \Delta B)$  at a depth of  $(d_r)$ , which is the vertical distance between the foundation level and the deepest reinforcement layer.

examined;  $l$  is the total length of reinforcement,  $N$  is the total number of reinforcement layers. The advantage of Hung and Menq is its relative simplicity in application, however it does not account for closeness of footings.

## 2. Experimental study

To validate a detailed numerical study program on different examined parameters, a number of experiments were conducted to determine the general trend of dependent parameters variation. A comparison will be performed between the experimental and numerical study on small scale model dimensions to guide a further extension of numerical investigation on prototype model dimensions.

### Materials and testing equipments

#### 2.1.1 Sand

Washed, air dried siliceous yellow sand was used in the model test. The sand was sieved through sieve No.4 with opening size of 4.75 mm. The specific gravity of soil particles was determined by the gas jar method. The main value determined from 3 tests was 2.66. The maximum and minimum dry unit weights of the sand were 18.22 and 15.45 kN/m<sup>3</sup>, respectively. The grain size distribution was determined using dry sieve method and the results are shown in Fig.2. From the grain size curve it was concluded that,  $D_{10}$ ,  $D_{30}$  and  $D_{60}$  were 0.3, 0.6 and 1.0 mm. Uniformity coefficient,  $C_u$  and coefficient of curvature,  $C_c$  were 3.3 and 1.14, respectively.

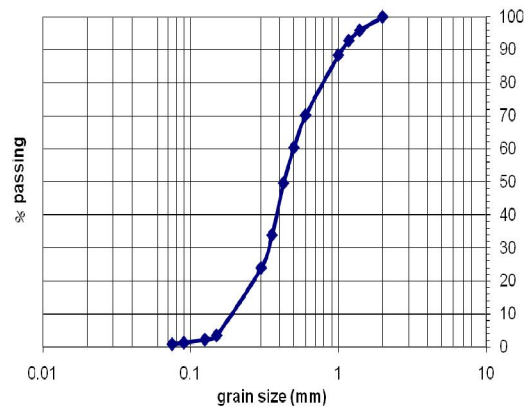


Fig.2 Particle size distribution of sand.

### 2.1.2 Geogrid reinforcement

The reinforcement material used in the present research is geogrid sheets known commercially as CE121 geogrid Fig.3. The polymer type from which sheets are manufactured is HD-polyethylene. Sheet dimensions are 2 m in width by 30 m in length, with thickness of 3.3 mm. The mesh aperture size is 8\*6 mm while the weight of unit area is 730 gm/m<sup>2</sup>. The mechanical properties as specified in the product data sheet is given in Table 1.



Fig. 3 Photographic view of Geogrid reinforcement.

**Table 1** Mechanical properties of geogrid reinforcement CE121

Mechanical property	
Tensile strength at maximum load	7.68 kN/m
Extension at max. load	20.2%
Load at 10% extension	6.8 kN/m
Elongation at ½ peak strength	3.22%
Axial stiffness, EA at 10% extension	6.8 kN/m

### 2.1.3 Sand container and loading mechanism.

Figure 4 illustrates a skethmatic representation of the sand container mounted under the loading frame with the hydraulic loading system. The tank dimensions are 500 \* 1200mm with a depth of 1000mm. One side of the tank was made of Perspex 10mm in thickness to observe the failure shape of model footings, while the other three sides together with the base were made of steel sheets 3mm in thickness. The steel sheets were stiffened by double back to back steel angles each 500 mm. A hydraulic jack of 50 kN maximum load capacity was used, the jack was mounted on a rigid broad flange I-beam (B.F.I.B) No. 10, and manually operated through a connected control unit. The reaction beam rests on and fixed to double box sections 50\*50 mm that are supported on the edges of the steel container at each end of the beam. The strip model was made of wood and has a dimension of 100mm in width, 500 mm in length and 150mm in thickness. The bottom and sides of the footing was covered by a sand paper to mobilize sufficiently the interface between footing and sand. A load distribution beam was mounted on the top of the adjacent stepped strip footings to distribute the hydraulic jack load equally on the two footings. Two dial gauges were mounted on the reaction beams above each footing to measure the resulting settlement (Fig. 4).

### 2.2 Experimental procedure

The sand was poured in the tank by sand raining technique keeping the height of fall as 400 mm in order to maintain constant relative density. The undrained shearing resistance of the sand due to such poring height results in a dry unit weight of 17 kN/m<sup>3</sup> and an angle of internal friction of 36° as determined using triaxial test. The tank was emptied and refilled after each test. The manually controlled hydraulic jack was used to apply the vertical load to a distributor beam which transmits the load equally on the two adjacent strip footings. The load was applied in increments until failure occurs. Reinforcement top layer level and extension was adopted according to optimum values recommended by Das et al. (1994). Settlement of each footing was measured trough a mounted dial gauge. The experimental investigation will be adopted to examine the adjacent footing effect for the cases of medium density soil and concentric loading only to verify the numerical model described below, different examined parameters including top reinforcement layer depth to footing breadth ratio (d/B), footing spacing to footing breadth ratio (s/B) as illustrated in Table (2). The numerical study will be extended to other values of previously mentioned and remaining tested parameters including internal friction of sand ( $\phi$ ), and load eccentricity. An outline

of the investigated problem and tested parameters is illustrated in Fig. 5.

To evaluate the capacity of an interfering footing on reinforced soil, the interference factor, BCR, may be defined as:

$$(BCR)_{\text{reinforced}} = q_{\text{int}(\text{reinforced})} / q_{\text{single}(\text{reinforced})}$$

$$(BCR)_{\text{unreinforced}} = q_{\text{int}(\text{unreinforced})} / q_{\text{single}(\text{unreinforced})}$$

Where:

$q_{\text{int}(\text{reinforced})}$  is the ultimate bearing capacity of interfering footing on reinforced soil;  $q_{\text{int}(\text{unreinforced})}$  is the ultimate bearing capacity of the footing on reinforced soil on unreinforced soil;

$q_{\text{single}(\text{reinforced})}$  is the ultimate bearing capacity of single footing on reinforced soil and

$q_{\text{single}(\text{unreinforced})}$  is the ultimate bearing capacity of single footing on unreinforced soil

Table 2 Experimental study cases.

Test No.	Description	s/B
1	Single strip footing on unreinforced sand	
2	Interfering footing on unreinforced sand	0
3		0.3
4		0.6
5		0.9
6		1.2
7	Single strip footing on reinforced sand	
8	Interfering footing on reinforced sand	0
9		0.3
10		0.6
11		0.9
12		1.2

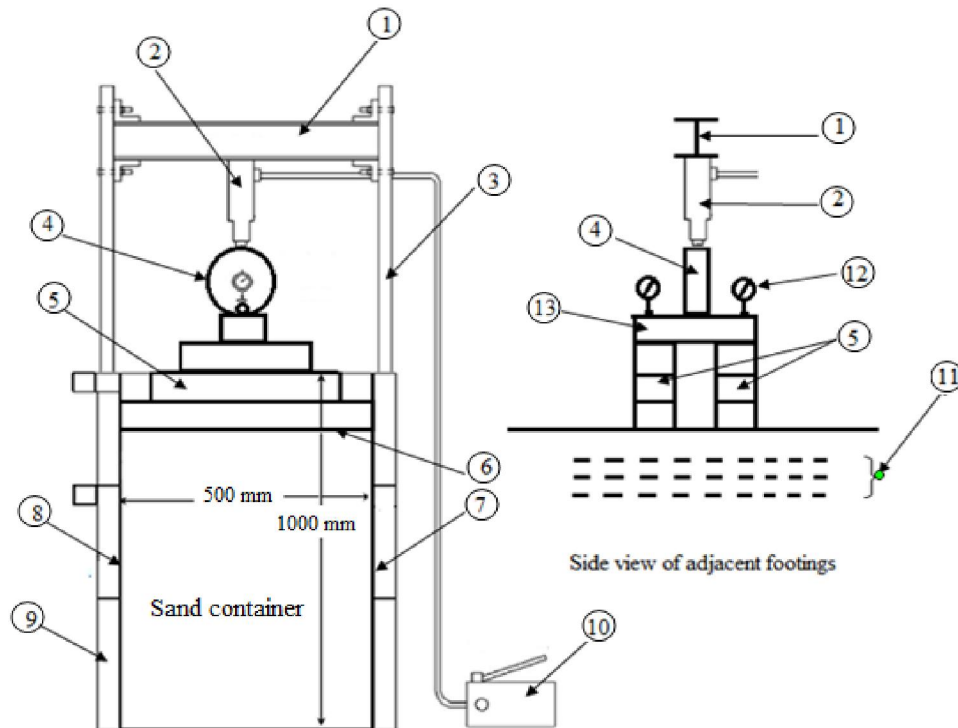


Fig. 4 Sketchmatic representation of experimental setup

Legend:

1- Reaction beam

4- Load ring

7- Perspex transparent side

10- Control unit of jack

13- Load distributor beam

2- Hydraulic jack

5- Stepped strip footing

8- Steel plate 3 mm

11- Geogrid reinforcement

3- Loading frame column

6- Foundation level

9- Stiffeners 2L 50\*5 mm

12- Dial gauge



Fig. 5 Photographic view of experimental study.

#### Numerical Model

Numerical models in this study were made using the finite element computer program called PLAXIS 3-D tunnel V1.2 (Bringgreve and Vermeer, 1998). The program has been verified by comparing solutions obtained from it with measurements taken

in actual case histories and studies. The program is able to simulate geogrid, sheets, soil and footings. The soil is modelled with 15-noded elements. Three dimensional model is used here to investigate the behaviour of two closely spaced strip footing. The dimensions of model are shown in Fig.6.

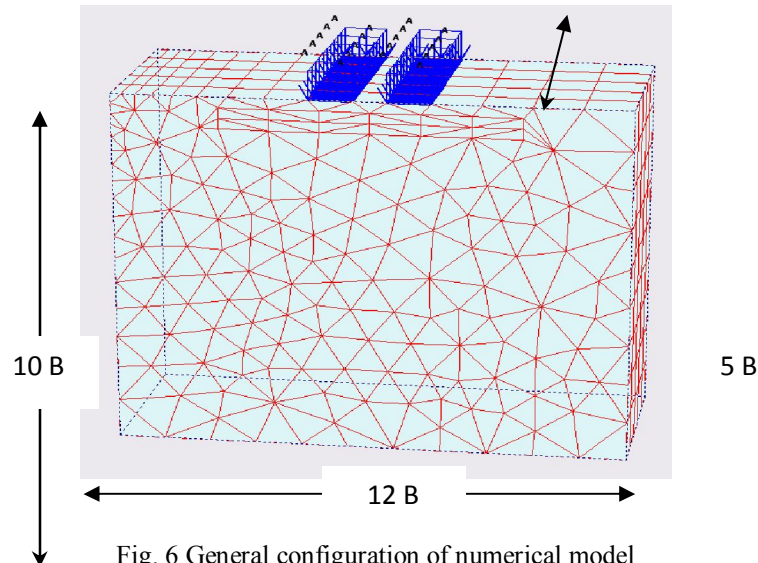


Fig. 6 General configuration of numerical model

These model dimensions were selected such that the magnitude of failure load remains unchanged even  $d$  is increased beyond the chosen value. The vertical boundaries of the model were constrained horizontally, and the bottom boundary was constrained in both horizontal and vertical directions. The parameters for footing and geogrid were assumed to maintain the same in all the finite element analyses. The analyses were used to reach the limit

loads (bearing capacity) for two parallel rough strip footings.

A Hardening-soil model is adopted in this numerical study to simulate the non-linear behavior of sand. Hardening-Soil model is the hyperbolic relationship between the vertical strain, and the deviatoric stress,  $q$ . In the special case of a drained triaxial test, the observed relationship between the axial strain and deviatoric stress can be well

approximated by a hyperbola as shown in Fig. 7. In this study the sand layer was dry and the initial effective stress was generated by means of  $k_0$  procedure. The limiting state of stress is described by means of the secant Young's modulus  $E_{50}^{ref}$ , the odometer modulus  $E_{oed}^{ref}$ , Poisson's ratio ( $\nu$ ), unloading reloading modulus, effective cohesion ( $c$ ), angle of internal friction ( $\phi$ ), angle of dilatancy ( $\psi$ ), failure ratio ( $R$ ) and interface reduction factor ( $R_{intf}$ ). A refined mesh is adopted to minimize the effect of mesh dependency on finite element modelling. The total number of nodes and elements in the model were 9610 and 1750, respectively. The reasonable parameters were assumed for medium dense sand in numerical analysis. It should be mentioned that the value of moduli ( $E_{50}^{ref}$ ,  $E_{oed}^{ref}$ ) had a small effect on the limit bearing capacity therefore, the values of  $E$  and  $\nu$  are kept constant in this study. These parameters were listed in Table 1. The reinforcing material (geogrid) used in this study was modelled as illustrated in table1. Geogrids layers can be activated or deactivated in the calculation phase using staged constructions as the loading input. The interaction between the geogrid and soil was modelled at both sides by means of interface elements which allow for the specification of a reduced wall friction compared to the friction of the soil and the interface reduction factor ( $R$ ) is taken as 0.8 and kept constant in all cases. The presence of interface element allows the relative movement taking place between reinforcement, footing and surrounding soil.

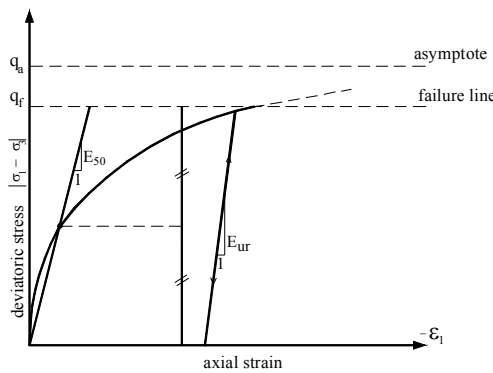


Fig. 7 Hyperbolic stress strain relation in primary loading for a standard drained triaxial test

The numerical model studied two identical strip footings each width  $B=1m$ , spaced by a distance  $s$  measured between their inside edges as shown in Fig.4. the bearing capacity is evaluated for rigid rough footing. The impediment of the footings can be taken into account through the surcharge  $q$ , i.e., the footing is placed at the ground surface with surcharge  $q = \gamma d$  where  $d$  is the embedment.

In this mechanism there is no slip between the soil and the footings, and the footings can be considered rough. To simulate a rigid rough footing, the horizontal displacements of nodes which discretize the footing, are constrained in the horizontal direction.

The footings are modelled as a plate element. The stiffness properties of footings section are: membrane “axial” rigidity,  $EA$ , and flexural rigidity,  $EI$ , are input as material properties. The plate is homogeneous and isotropic, in the sense that, everywhere in the plate, the membrane and flexural rigidity parameters (per unit length) do not change with direction. For numerical calculations, an equivalent thickness for the plate ( $d_{eq}$ ) is calculated based on values of its rigidity parameters,  $EI$  and  $EA$  as

$$d_{eq} = \sqrt{12 \frac{EI}{EA}} \tag{4}$$

**4 Verification**

Figure 8 shows the comparison of results obtained by the numerical analysis based on Plaxis and that obtained by the experimental study. These results corresponds to the case of  $d=0$ , and uniform centric load. It can be seen that the numerical prediction from the numerical study seems reasonable and agrees reasonably with the measured results.

**5. Parametric study**

The geometry of the model in this investigation was shown in Fig. 9. The parametric study included changing of friction angle ( $\phi$ ), the impediment depth ( $d$ ), the spacing between interfering strip footing ( $s$ ) and the ratio ( $r=q_1/q_2$ ) to simulate the load eccentricity. The parameters  $d$  and  $s$  are normalized to footing width ( $B$ ). Table 3 shows the various cases that included in the numerical study.

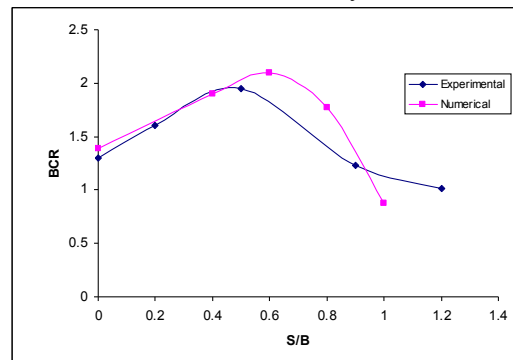


Fig. 8 comparison of numerical and experimental study for interfering strip footing for case of  $\phi=35$ ,  $d/B=0$ .

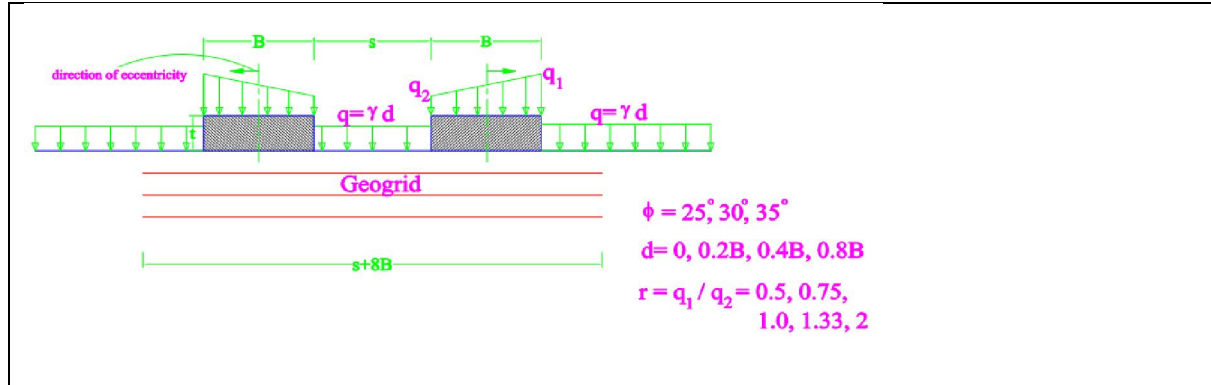


Fig. 9 problem Outline

## 6. Analysis and Results

### 6.1 influence of angle of internal friction of soil ( )

Numerical analyses were performed on interfering strip footings placed on unreinforced and reinforced sand with three layers of geogrid.

Large scale strip footing is analysed with  $B=2\text{m}$ . The relation between (BCR) and  $(s/B)$  for relative depth  $(d/B) = 0$  i.e. at ground level surface, is illustrated in Fig.10 for unreinforced soil case with different angles of internal friction  $\phi = 25, 30$  and  $35^\circ$ . It can be observed that (BCR) ratio increases with increase of  $(s/B)$  ratio up to a footings spacing of nearly one half footing breadth i.e. at  $(s/B) = 0.4$  for  $\phi = 25^\circ, 30^\circ$  and  $(s/B) = 0.6$  for higher soil density at  $\phi = 35^\circ$ . With further increase of footings spacing up to a value equaling the footing breadth  $(s/B = 1.0)$  a

reduction occurs in (BCR) ratio with increase of  $(s/B)$  ratio. As relative footing spacing exceeds 1.0, (BCR) decreases linearly with a relatively smaller rate and it can be said that the two strip footing behave as a single footing. The previously described trend of the relation between (BCR) and  $(s/B)$  ratios applies for different adopted values of angle of friction including  $25, 30$  and  $35^\circ$ . The (BCR) increases for in between footing spacing ranging from zero to as time as footing breadth as frictional angle increase where the maximum (BCR) equal to 2.15, 1.7 and 1.4 for  $25^\circ, 30^\circ$  and  $35^\circ$  respectively. This general trend applies also for the reinforced soil case as can be seen in Fig. 11. For the case of zero in between footing spacing of the reinforced soil case, no significant deference in bearing capacity (BCR) ratio can be observed.

Table 3 Parameters investigated in the numerical study.

Group*	Constant parameters	Variable parameters	Remark
1	$d=0.0, r=1$	$\phi = 25^\circ, 30^\circ, 35^\circ$ $s/B=0, 0.2, 0.4, 0.6, 0.8, 1.0$	Influence of angle of friction (18 cases)
2	$\phi = 25^\circ, r=1$	$d/B = 0, 0.2, 0.4, 0.6$ $s/B=0, 0.2, 0.4, 0.6, 0.8, 1.0$	Influence of impediment depth (24 cases)
3	$\phi = 25^\circ, d=0$	$r=1, 1.33, 2, 4$ $s/d=0, 0.2, 0.4, 0.6, 0.8, 1.0$	Influence of load eccentricity (24 cases)

\* Groups are analysed for reinforced and unreinforced sand

It can be observed that as the spacing between the two adjacent footings exceeds footing breadth the closeness effect of the footings vanishes i.e. (BCR) equals 1.0. Except for the case of zero footings spacing of reinforced soil case it can be observed that (BCR) increases with increase of angle of internal friction up to relative footing spacing  $(s/B)$  equaling 1.0. It can be also concluded that existence of two footings adjacent to each other rise their bearing capacity compared to single footing case for both unreinforced and reinforced cases for different in between spacing and soil densities. This applies for the cases of in between footing spacing ranging from zero to two times footing breadth for the unreinforced

soil case and zero to one times footing breadth for the reinforced soil case. This may be attributed to the arching effect of soil between the adjacent footings. As concerning the effect of reinforcement on soil arching related to the angle of friction it is clear from the two previously presented figures that at an inbetween spacing resulting in the maximum interfering effect (0.4-0.6) the ratio between (BCR) for the reinforced and unreinforced cases are 1.38, 1.28 and 1.18 for angles of friction of  $25, 30$  and  $35^\circ$ , respectively. This reflects that the reinforcement is more significant in improving the soil arching between adjacent footings with the case of more loose foundation soil.

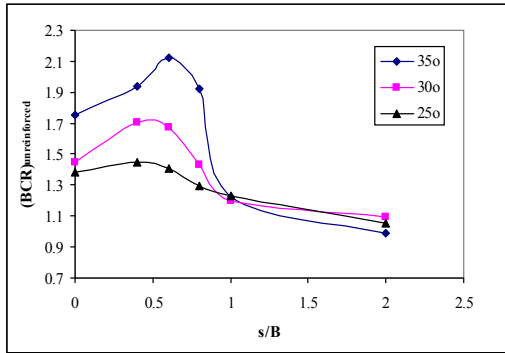


Fig. 10 Relation between (BCR) and (s/B) for unreinforced soil case.

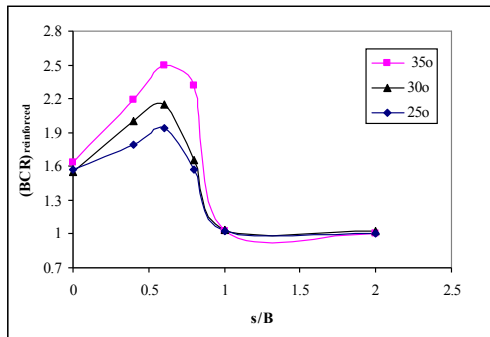


Fig. 11 Relation between (BCR) and (s/B) for reinforced soil case.

## 6.2 Influence of internal foundation depth (d)

Figure 12 illustrates the relation between (BCR) and (s/B) ratios for different relative foundation depths for the unreinforced soil case with relative foundation depth ( $d/B$ ) ranging from 0 to 0.8, for the loosest considered soil case ( $\phi = 25^\circ$ ). Reflecting the same trend as that observed with relative foundation depth ( $d/B = 0$ ), (BCR) ratio increases with increase of (s/B) ratio until reaching a value of 0.4. For deeper foundation depth ( $d/B = 0.2$  to 0.8). A decrease in (BCR) ratio can be observed with further increase in (s/B) ratio. In case of relatively deep foundation level of ( $d/B = 0.8$ ), (BCR) seems to be unchanged with increase of in between footings spacing equaling footing breadth. It can be also concluded that the closeness of footings is more effective in raising carrying capacity of soil due to soil arching as the foundation depth increases, the recorded (BCR) was 1.15, 1.32 and 1.58 as times as corresponding value recorded with ( $d/B = 0$ ) for deeper foundation depth of 0.2, 0.4 and 0.8, respectively.

As for the reinforced soil case as illustrated in Fig. 12, the general trend of the (BCR) and (s/B) ratios for different ( $d/B$ ) can be described as having the same trend as that observed with the unreinforced case except that the maximum (BCR) ratio is shifted towards a higher (s/B) ratio of 0.6 for ( $d/B = 0$ ), 0.2 and 0.4.

Maximum (BCR) is shifted to an (s/B) ratio of 0.8 for ( $d/B = 0.8$ ). Rather than the moderate decrease in (BCR) ratio with increase of relative footings spacing ratio from 0.5 to 1.0 in the unreinforced case a more steep reduction is observed with the reinforced case. It can be also observed from Fig.9 reinforcement of soil seems to retain the same (BCR) with increase of (s/B) ratio of more than 1.0 up to footing spacing as more as two times footing breadth. For deeper foundation level, soil reinforcement seems to have a smaller effect on (BCR) compared to unreinforced case, i.e. the (BCR) increases by 1.06, 1.13 and 1.38 for relative foundation depth ( $d/B$ ) of 0.2, 0.4 and 0.8, respectively.

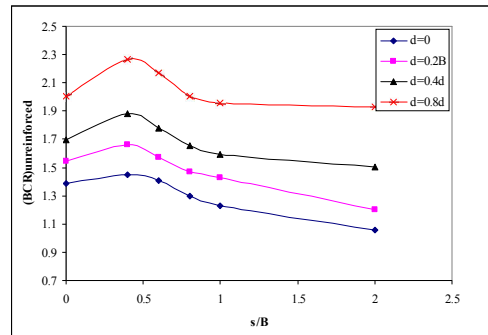


Fig. 12 Relation between (BCR) and (s/B) for unreinforced soil case for different relative foundation depths.

## 6. Influence of load nonuniformity (r)

Fig. 13 shows the relation between (BCR) and spacing between interfering footings for different value of  $r$  for case of reinforced sand. it can be seen that the (BCR) increases as the ratio  $r$  increase whereas the maximum values of (BCR) are 1.93, 2.17, 2.45 for  $r=1, 2, 3$  respectively. Also the direction of eccentricity about the center of footing do not affects (BCR) i.e (BCR) for  $r=2$  is equal to that for  $r=0.5$ . The previous trend can be observed for the case of unreinforced sand as shown in Fig. 14.

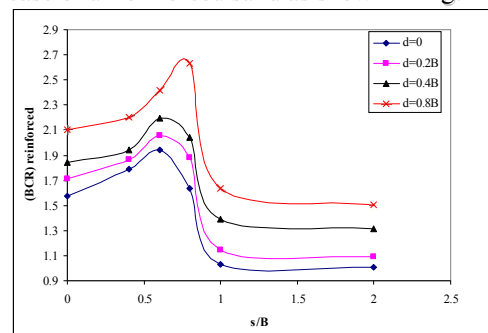


Fig. 13 Relation between (BCR) and (s/B) for reinforced soil case for different relative foundation depths.

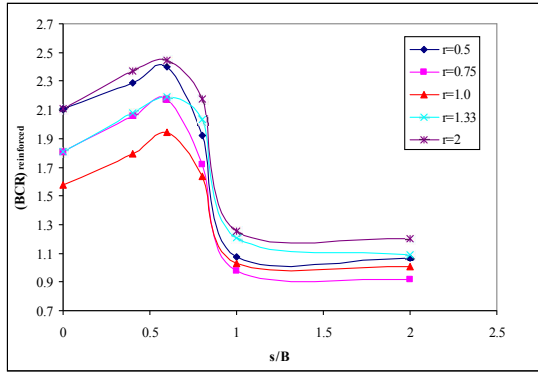


Fig. 14 Effect of load nonuniformity on (BCR) for unreinforced sand

The previous trend can be observed for the case of unreinforced sand as shown in Fig. 12. It can be noted that the (BCR) slightly affected by the direction of load eccentricity.

**6.4 Inclusion of interfering effect in Huang and Menq (1997) equation**

By backwards substitution in Huang and Menq equation (1997) a factor ( $R_{unrein}$ ) and ( $R_{rein}$ ) may be introduced to the increase or decrease of footing width  $\Delta B$  for the cases of unreinforced and reinforced soil, respectively. The equation may be represented as follows:

For a strip footing resting on unreinforced soil:

$$q_{(unrein)s} = \zeta * (R_{unrein}) * B * N + d * N_d \quad (4)$$

For a strip footing resting on reinforced soil:

$$q_{(rein)s} = \zeta * (B + (R_{rein}) * \Delta B) * N + d * N_d \quad (5)$$

where

$$R_{unrein} = \mu_{1u} * (s/B)^2 + \mu_{2u} * (s/B) + \mu_{3u} \quad (6)$$

$$R_{rein} = \mu_{1r} * (s/B)^2 + \mu_{2r} * (s/B) + \mu_{3r} \quad (7)$$

Factors of the two previous equations of the unreinforced soil case  $\mu_{1u}$ ,  $\mu_{2u}$ ,  $\mu_{3u}$  and the reinforced soil case  $\mu_{1r}$ ,  $\mu_{2r}$ ,  $\mu_{3r}$  may be expressed in a general form by the following equation.

$$\mu = F_1 * (d/B)^3 + F_2 * (d/B)^2 + F_3 * (d/B) + F_4 \quad (8)$$

Factors  $F_1$ ,  $F_2$ ,  $F_3$  and  $F_4$  for the relatively loose soil case with angle of internal friction  $\phi = 25^\circ$  may be expressed in Table 4.

Table (4) Factors  $F_1$ ,  $F_2$ ,  $F_3$  and  $F_4$ .

		$\mu_1$		$\mu_2$		$\mu_3$	
		unrein.	rein	unrein.	rein	unrein.	rein
F1	$0 \leq d/B < 0.6$	-1.317	-97.6	-2.135	60.78	-4.526	-30.35
	$0.6 \leq d/B < 1$	10.56	185.3	-25.46	-322.4	9.729	97.72
F2	$0 \leq d/B < 0.6$	1.753	115.7	2.481	-73.02	5.665	38.12
	$0.6 \leq d/B < 1$	-11.23	-234	26.21	402.9	-8.437	-121.5
F3	$0 \leq d/B < 0.6$	-0.672	-32.67	-0.4	20.78	-1.672	-11.01
	$0.6 \leq d/B < 1$	2.145	20.78	-4.66	-111.9	0.598	32.67
F4	$0 \leq d/B < 0.6$	0.16	4.017	0.001	4.017	0.771	5.895
	$0.6 \leq d/B < 1$	0.491	-0.107	-1.075	14.03	1.298	4.014

**Conclusions**

An experimentally verified by numerical study were conducted to examine the interfering effect on performance of adjacent strip footings. The study included examining the effect of spacing in between footing, foundation depth and load nonuniformity on both unreinforced and reinforced sand. It is concluded that interfering footing results in increasing bearing capacity ratio compared to the single strip footing case. The interfering effect reaches it maximum at relative footing spacing of nearly one half footing breadth. As the relative footing spacing exceeds footing breadth the interfering effect vanishes. The ratio of bearing capacity of interfering footings to that of single footing increases as the density of sand increases for in between footing spacing of less than footing breadth. Sand reinforcement was observed to enhance the interfering effect of adjacent footings. The interfering effect increases with increase of foundation depth and the enhancement is more effective in case of unreinforced sand. The bearing capacity ratio increases as the load nonuniformity ratio increases with slightly higher effect in case of reinforced sand compared to the unreinforced foundation soil case. The interfering effect of closely spaced footings for unreinforced and reinforced sand may be included in equations of determining bearing capacity of single strip footing.

**Corresponding author**

**Ahmed F. Zidan**

Structural Engineering Department, Faculty of Engineering, Beiny Suafe University, Egypt.

[Ahmedzidan2008@gmail.com](mailto:Ahmedzidan2008@gmail.com)

**References**

1. Alamshahi S, Hataf N. "Bearing capacity of strip footings on sand slopes reinforced with geogrid and grid-anchor". *Geotext Geomembr* 2009; 27(3):217-226
2. Bathurst RJ, Nernheim A, Walters DL, Allen TM, Burgess P, Saunders DD. "Influence of reinforcement stiffness and compaction on the performance of four geosynthetic-reinforced soil walls". *Geosynth Int* 2009 16(1):43-49
3. Chung W, Cascante G. "Experimental and numerical study of soil reinforcement effects on the low strain stiffness and bearing capacity of shallow foundations". *Geotech Geol Eng* 2007; 25:265-281
4. Das, B. M., Shin, E. C., and Omar, M. T. "The bearing capacity of surface strip foundation on geogrid reinforced sand and clay - a comparative study", *Geotechnical and Geological Engineering* 1994; Vol. 12, pp. 1-14.

5. Das BM, Larbi-Cherif S. "Bearing capacity of two closely-spaced shallow foundations on sand". *Soils Found* 1983; 23(1):1–7.
6. Graham J, Raymond GP, Suppiah A. "Bearing capacity of three closely-spaced footings on sand". *Géotechnique* 1984;34(2):173–82.
7. Ghazavi, M., and Lavasan, A., "Interference Effect of Shallow Foundations Constructed on Sand Reinforced with Geosynthetics," *Geotextiles and Geomembranes*, Vol. 26, 2008, p. 407.
8. Khing, K.H., Das, B.M., Yen, S.C., Puri, V.K. and Cook, E.E. "Interference effect of two closely-spaced strip foundation on geogrid-reinforced sand", *Geotech. And Geological Engrg. Jl.* 1992a, Chapman and Hall, London.
9. Lovisa J, Shukla SK, Sivakugan N. "Behaviour of prestressed geotextile-reinforced sand bed supporting a loaded circular footing". *Geotext Geomembr* 2010; 28(1):23–32
10. Vinod P, Bhaskar AB, Sreehari S. "Behaviour of a square model footing on loose sand reinforced with braided coir rope". *Geotext Geomembr*; 2009 27(6):464–474
11. PLAXIS 3D tunnel program. Reference manual, version 1.2; 2000.
12. Schlosser, F., Jacobsen, H. M. and Juran, I. . "Soil Reinforcement." *Proc., 8<sup>th</sup> ECSMFE*, Helsinki, Finland (1983); 1180-1159
13. Tafreshi SN, Dawson AR. "Behaviour of footings on reinforced sand subjected to repeated loading—Comparing use of 3D and planar geotextile". *Geotext Geomembr* 2010; 28(5):434–447
14. Zidan AF. Numerical study of Behavior of circular footing on geogrid-reinforced sand under static and dynamic loading" *Geotechnical and Geological Engineering* 2012; 30 (2): 499-510.
15. Terzaghi K. *Theoretical soil mechanics*. New York: Wiley; 1943.
16. Stuart JG. Interference between foundations, with special reference to surface footings in sand. *Géotechnique* 1962; 12(1):15–22.
17. Saran S, Agarwal VC. "Interference of surface footings on sand". *Indian Geotech J* 1974;4(2):129–39.
18. Huang, C. And Menq, F., "Deep-footing and wide slab effects in reinforced sandy ground", *Journal of Geotechnical Engineering*, ASCE 1997, Vol. 123, No. 1, pp. 30-36.
19. Kumar A, Saran S. "Closely spaced footings on geogrid-reinforced sand". *J Geotech Geoenviron Eng ASCE* 2003; 129(7):660–4.
20. Kumar J, Ghosh P. "Ultimate bearing capacity of two interfering rough strip footings". *Int J Geomech ASCE* 2007; 7(1):53–62.
21. Kumar J, Kouzer KM. "Bearing capacity of two interfering footings". *Int J Numerical Methods Geomech* 2008;32:251–64.
22. Kumar J, Bhoi MK. "Interference of two closely spaced strip footings on sand using model tests". *J Geotech Geoenviron Eng ASCE* 2008; 134(4):595–604.
23. Kouzer KM, Kumar J. "Ultimate bearing capacity of equally spaced multiple strip footings on cohesionless soils without surcharge". *Int J Numer Anal Methods Geomech* 2008; 32:1417–26.

12/20/2012